



Grafting and characterization of dodecylphosphonic acid on copper: Macro-tribological behavior and surface properties

Mohamed Moustapha Moine^a, Xavier Roizard^a, Jean-Marie Melot^b, Luc Carpentier^a, Pierre-Henri Cornuault^a, Fabrice Lallemand^{b,*}, Jean-Marie Rauch^a, Olivier Heintz^c, Séverine Lallemand^b

^a Institut FEMTO-ST, UMR 6174 CNRS, Université de Franche-Comté, 26, Chemin de l'Épitaphe, 25030 Besançon Cedex, France

^b Institut UTINAM, UMR 6213 CNRS, Université de Franche-Comté, 30 Avenue de l'Observatoire, 25009 Besançon Cedex, France

^c ICB Laboratory, UMR 6303 CNRS, Université de Bourgogne, 9, Av. Alain Savary, 21078 Dijon Cedex, France

ARTICLE INFO

Article history:

Received 15 March 2013

Accepted in revised form 8 June 2013

Available online 14 June 2013

Keywords:

Self-assembly process

Phosphonic acid

Copper oxide

Sonication

Corrosion

Tribology

ABSTRACT

Thin film of n-dodecylphosphonic acid (DDPA) was prepared on a copper oxide substrate via a molecular self-assembly process. The composition, structure, organization, surface energy, morphology, and electrochemical behavior of the DDPA film were characterized by means of X-ray photoelectron spectroscopic analysis (XPS), polarization modulation infrared reflection absorption spectroscopy (PM-IRRAS), contact angle measurement (CAM), microscopic observations, and electrochemistry. The friction behavior of the DDPA film adsorbed on copper oxide substrate sliding against a Si₃N₄ ball was examined on a linear reciprocating tribological tester. Worn surfaces of the DDPA film were observed with a scanning electron microscope. All properties of the DDPA film were compared and discussed in terms of sonication effects just after surface functionalization. The presence and organization of alkyl phosphonate molecule on Cu were confirmed by XPS, PM-IRRAS and CAM analyses. PM-IRRAS data gave some indication of tridentate bonding between phosphonic groups and oxidized Cu surface. Electrochemical studies showed strong anti-corrosion behavior. Excellent tribological behavior was observed for DDPA film before sonication (DDPA/Cu BS) under contact pressure of 133 MPa and low sliding speed of 1 mm·s⁻¹ conditions. In the case of DDPA/Cu BS surface, very low friction coefficient value ($\mu \approx 0.12$) and increase in antiwear life (100 times higher) were observed, compared to a DDPA film after sonication (DDPA/Cu AS) and a bare Cu substrate.

© 2013 Elsevier B.V. All rights reserved.

1. Introduction

Metal forming processes of sheet components such as rolling, cutting, stamping, embossing, are widely used for various applications employed in important industrial sectors (automotive, aircraft, energy production, building and electronic devices). During metal elaboration, mechanical stresses are transmitted from the tool to the shaped metal sheet, and sliding between these two parts should be facilitated. In order to perfect processes in terms of energy consumption and cost limitation, one obvious objective is to minimize friction and wear of tool/sheet contacts. This point is particularly important in order to assure tool integrity, as far as used metal sheets are generally oxidized in a way that fine and very hard metal oxide particles could be trapped at the tool/metal sheet interface, tending to promote abrasion wear mechanisms. In this way, one common technique to protect surfaces and to limit friction forces is to employ oil-based lubricants, which should be selected depending on forming process parameters such as tools, sheet materials' nature and composition, sliding speed, temperature, and normal load. Nevertheless, classical lubricants have two main

drawbacks resulting in additional expenses. First, optimization of the lubricant amount is difficult to reach, because of both tool and sheet roughness on one side and lubricant's high viscosity on the other side. These difficulties lead to over-consumption of the later to assure contact lubrication. Second, in most cases the lubricant has to be removed from the metal sheet after forming; thus subsequent cleaning operations have to be performed, leading to additional and undesirable costs.

Consequently, an eventual replacement of metal sheet and tool lubrication method could be of great interest in order to limit forming process costs. Thus, one idea is to functionalize metal sheet surfaces with Self-Assembled Molecules acting as an eventual lubricant. Self-Assembled Monolayers (SAMs) allow the production of functionalized surfaces based on grafting of organic molecule film by means of a chemical reaction, leading to chemisorption of molecules on the substrate. This physicochemical surface modification method offers several advantages, since it is easier to implement than other existing coating techniques. Indeed, spontaneous film is formed on the surface by simply immersing the substrate in a weakly concentrated solution of reactive molecules dispersed in a solvent without any external energy supply. Note that the solvent used in this study (high purity ethanol) is a limiting factor in terms of industrial applications, but classical 95% ethanol solution could be used as well, leading to cheaper experiments.

* Corresponding author. Tel.: +33 3 81 66 68 63; fax: +33 3 81 66 68 58.

E-mail address: fabrice.lallemand@univ-fcomte.fr (F. Lallemand).

Moreover, the sharpness of SAMs produced (nanometer scale thickness) avoids subsequent cleaning operation.

While grafting quality is highly dependent on the nature of both molecules and substrate, SAM/substrate systems are claimed to form highly organized films on metal oxide surfaces including alkylphosphonic acids on steel, stainless steel, brass, aluminum, copper, passivated Ni–Ti and cobalt chromium (Co–Cr) alloy [1–6], arachidic acid on Al_2O_3 thin film [7], n-alkanoic acids on natively oxidized Al, Cu and Ag [8,9], fatty acids on steel [10], octadecylsilane on Al_2O_3 [11] and alkanethiol on Ni, Ag and Cu [12–15]. Due to their low toxicity, alkylphosphonic acids could be destined to replace former SAMs like organothiols or organoselenols derivatives. The grafting mechanism of alkylphosphonic acid molecules is generally described as an acid–base reaction between the SAM's phosphonic groups and the hydroxyl groups present on copper surface [3]. Although a large number of studies described the reaction mechanism as a covalent bond formation, the number of so-formed bonds is actually highly dependent not only on the substrate properties, but also on the molecular grafting mode which could be mono-, bi- or tridentate.

SAMs have been the topic of extensive research, both for their fundamental importance in understanding interfacial properties as well as their potential applications in corrosion resistance, catalysis, biological sensors, adhesion systems, protein films, electronic devices fabrication etc. [14–24]. Nevertheless, few papers have been suggested to assess the tribological behavior and efficiency of such SAMs [3,10,15]; moreover, tribological tests are usually carried out using a nanotribometer, which is also not representative of the real metal sheet/tool contact scale [3].

In the present work, n-dodecylphosphonic acid (DDPA) synthesized in our laboratory is used as a reactive group to form SAM films on copper oxide substrates in order to investigate the tribological efficiency of this surface modification route in the case of forming processes used in microelectronic industrial sector (cutting, stamping ...). Specimens employed in this study are CuA1 copper (99.9% Cu). In the first part, SAMs' composition, structure and organization are characterized by spectroscopic techniques. Results stemming from electrochemical techniques are presented, revealing oxidation blocking factor and anti-corrosion properties of SAMs. In the second part, the influence of surface modification on friction and wear behavior is studied by means of tribological experiments. The effects of sonication on DDPA films in terms of chemical and tribological properties are then investigated. Thereafter, functionalized copper substrates with DDPA film before and after ultrasonic cleaning will be called DDPA/Cu BS and DDPA/Cu AS, respectively.

2. Experimental section

2.1. Chemicals

De-ionized water (Milli-Q, resistivity $18 \text{ M}\Omega \cdot \text{cm}$) was distilled twice before use. 1-Bromododecane (ALFA AESAR, 98 %, 143–15-7), triethylphosphite (ALFA AESAR, 98%, 122–52-1), perchloric acid (ACROS, 70%, 7601–90-3), sulfuric acid (ACROS, 96%, 7664–93-9), absolute ethanol (ACROS, pure, 64–17-5), sodium hydroxide (ACROS, 97+%, 1310–73-2) and sodium chloride (ACROS, extra pure, 7647–14-5) were used as received. ^{31}P NMR spectrum was performed from a Bruker AC 300 apparatus, using a solution in CD_3SOCD_3 with 1 M H_3PO_4 as an external standard. Mass spectrum was obtained from a LTQ Orbitrap apparatus with a negative ESI source.

1-Bromododecane (50.0 g, 200 mmol) was heated to 200°C (oil bath). Triethylphosphite (45.0 g, 240 mmol) was added dropwise during 30 min., whereas bromoethane was continuously distilled-off (vapor temperature below 40°C). The mixture was then brought to $220\text{--}225^\circ\text{C}$ and maintained at this temperature until the distillate flow slowed down (30–40 min.) Excess triethylphosphite was eliminated at 50–100 mm Hg for 5–10 min and the resulting oil cooled to

room-temperature. Concentrated aqueous hydrochloric acid (12 M, 250 mL) was added and the heterogeneous mixture stirred and boiled (100°C) for 15 h. After cooling to room-temperature, the semi-oily mixture was extracted with dichloromethane ($2 \times 100 \text{ mL}$). After drying (anhydrous sodium sulfate), the organic phase was concentrated (60°C , 400 mm Hg) to an oil, which soon solidified. It was recrystallized from cyclohexane to afford off-white plates.

Yield: 74%. F: 99°C . ^{31}P NMR (121.45 MHz, 300 K): $\delta = 27.4 \text{ ppm}$. MS (C = 10^{-5} M in methanol): exact mass ($\text{g} \cdot \text{mol}^{-1}$): 249.1641; Found: 249.1666.

2.2. Pretreatment of the working electrode

Copper substrates were cut into $20 \text{ mm} \times 20 \text{ mm}$ pieces, without additional polishing. The copper surfaces were sonicated in absolute ethanol and ultra-pure water for 5 min and then electrochemically reduced in 0.5 M aqueous perchloric acid under a current of $-800 \mu\text{A}/\text{cm}^2$ for about 120 s, until metallic copper potential was attained ($< -720 \text{ mV}/\text{SCE}$). The samples were cleaned again in aqueous nitric acid solution (pH = 1.8) for 7 min and oxidized by exposure to a 5% aqueous hydrogen peroxide (H_2O_2) solution for 10 min at room temperature.

2.3. Monolayer preparation

The SAMs were grafted by dipping the oxidized copper surface in a 10^{-3} M solution of dodecylphosphonic acid (DDPA) in absolute ethanol for 16 h under argon flow. The surface was then rinsed with absolute ethanol. Subsequently, a first class of samples (called DDPA/Cu AS) was cleaned in a sonication bath for 5 min to remove physisorbed species, while a second group of samples (called DDPA/Cu BS) had no other post-treatment. Samples were kept in inert atmosphere until characterizations were completed. The sample preparation procedure used for this study was identical to that used for previous studies [3,4].

2.4. Surface characterization

2.4.1. XPS

In this study, XPS is used to measure elemental composition in order to determine oxidation state of elements. Two different XPS equipments were used in this study. The first one was used for depth profiling of oxidized copper surface and the second one was used to analyze the SAM surface after functionalization tests, just in order to focus the grafting quality. All spectra for depth profiling were acquired using monochromatized Al K α radiation (1486.6 eV). X-ray radiation source operated in ultrahigh vacuum (UHV) (base pressure below 10^{-11} mbar). The load lock chamber was pumped down to 10^{-6} mbar with a primary rotative pump and a secondary turbo molecular one. The main chamber was pumped down to 10^{-11} mbar with titanium sublimation pump and an ionic one. The binding energies of the cores levels were calibrated in function of the C 1 s binding energy set at 285.5 eV, a characteristic energy of alkyl moieties, and deconvolutions were made using mixed Gaussian–Lorentzian curves (80% of Gaussian character).

The surface chemical state of Cu samples just before functionalization after chemical tests was analyzed by an X-ray photoelectron spectroscopy (XPS). All binding energies were corrected to a carbon C 1 s binding energy of 285.5 eV to reduce the charging effects. All the oxidized samples were first pumped down to 10^{-6} mbar in a load lock vacuum chamber in order to degas the surface. Then the entire samples were introduced into the main chamber for analyses. The analyses were realized in several alternative levels of X-ray measurements and etching time in order to detect elements of the surface from the top layer to the bulk of the oxidized copper substrate. The etching step was realized using an ion argon gun with a tungsten filament and differential vacuum system in order to sputter pure argon ion in the chamber, through

a shadow, under a vacuum pressure of 5.10^{-8} mbar. The etching time was 400 s, and we have realized 7 levels of analyses/etching during this experiment. X-ray measurements were realized with Al K α electron under a vacuum of $3 \cdot 10^{-9}$ mbar.

2.4.2. PM-IRRAS

Polarization Modulation Infrared Reflection Absorption Spectroscopy data were collected from a Bruker VERTEX 70 PMA 50 equipped with a liquid-nitrogen-cooled mercury-cadmium-telluride (MCT) detector and a photoelastic modular PMA: ZnSe. The infrared light, reaching the sample surface at an angle of 75° , was modulated between s- and p-polarizations at a frequency of 50 kHz. Signals generated from each polarization (Rs and Rp) were detected simultaneously by a lock-in amplifier and used to calculate the differential surface reflectivity $\Delta R/R = (R_p - R_s) / (R_p + R_s)$. The spectra were taken by collecting 974 scans with a spectral resolution of 2 cm^{-1} .

2.4.3. Surface energy

In order to evaluate surface energies, the steady-state advancing contact angles of different liquids droplets ($10 \mu\text{l}$) formed were measured at room temperature by a contact angle analyzer (I.T.CONCEPT, France). The polar (γ_s^h) and nonpolar component (γ_s^d) of the surface

energy were evaluated by the application of the following Owens and Wendt equation [25]:

$$1 + \cos\theta = \frac{2 \left[\sqrt{\gamma_s^d \gamma_l^d} + \sqrt{\gamma_s^h \gamma_l^h} \right]}{\gamma_{lv}} \quad (1)$$

where θ , γ_{lv} , γ_l^d and γ_l^h denote the advancing contact angle, the liquid surface tension, the nonpolar and the polar components of the liquid surface tension, respectively. Since γ_l^d and γ_l^h were reported in the literature [25], γ_s^d and γ_s^h were readily evaluated from the measured θ value by solving Eq. (1).

2.4.4. Electrochemical characterization

Electrochemical characterization was carried out using a VoltaLab 40 PGZ 301 potentiostat (Tacussel-Radiometer Analytical SA-France) controlled by a computer via VoltaMaster 4 Software interface. The used three electrode setup consisted of a saturated calomel reference electrode (SCE), a platinum counter-electrode and the modified copper working electrode. Cyclic voltammetry studies were performed in a 0.1 M NaOH aqueous solution at a scan rate of 20 mV s^{-1} between -1 and 0.4 V/SCE . Polarization curves were obtained in a 0.5 M NaCl solution under a 5 mV s^{-1} scan rate.

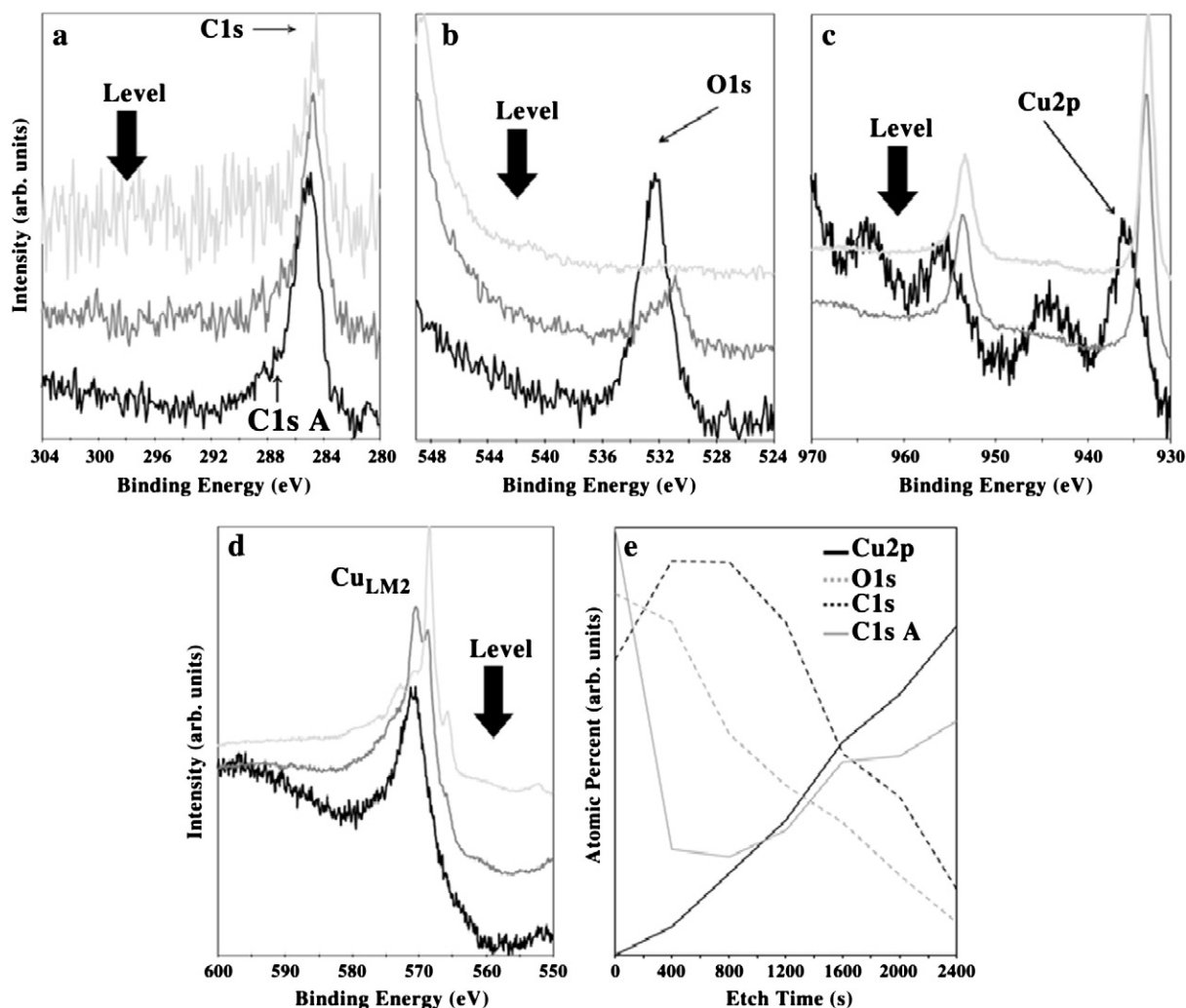


Fig. 1. XPS spectra (15 scans, $0 \mu\text{m}$, CAE 20.0, 0.10 eV) of bare oxidized copper for core level (a) C 1s, (b) O 1s, (c) Cu 2p and (d) LM2 Auger Cu with all etching levels and (e) atomic percent profile (15 scans, $0 \mu\text{m}$, CAE 20.0). Full arrow shows the decreased direction from the etching level (6, 3 to 0).

2.4.5. Tribological measurements

To explore tribologic properties, we studied the response of bare copper and SAMs modified copper before and after cleaning with ultrasounds. Using a microtribometer, tribological tests were performed on a reciprocating self-made tribometer with pin on disk geometry at room temperature. The mechanical setup is presented in [15].

The structure of this tribometer could be divided in three functional sub-systems:

- The mechanical arrangement ensuring the relative displacement between the pin and the disk and carrying the required contact load out,
- The measuring head, which allows the monitoring of tribological parameters,
- The control and data acquisition system used for driving the tribometer and for data acquisition and processing. The treatment of measurements and the display of the results are gained by homemade software.

The general features of this device could be summarizing as follows:

- The static normal load could be adjusted in the range of few tenths to few hundreds mN.
- The sliding displacement is given by an alternative motion at constant speed (triangular driving displacement signal), the oscillating frequency varying from 0.1 to 4 Hz.
- The magnitude of the displacement reaches values from 10 μm up to 1 mm with a theoretical lateral resolution of 0.1 μm .

After theoretical calculation by means of Hertz contact theory, a 20 mm diameter Si_3N_4 ball was used as friction pin with a normal load of 0.2 N. Thus, the theoretical maximum pressure under contact was $p_0 = 133$ MPa. It is worth noting that silicon nitride (Si_3N_4) ball has been selected due to high stiffness and hardness (315 GPa and 1600 HV), chemical inertia of the material and surface low-roughness ($R_a = 0.04$ μm) obtained after processing.

The sliding velocity and length were 1 mm/s and 1 mm. The friction coefficient was an average of five test results and the standard deviation was calculated.

2.4.6. Morphological observations

The surface topography of DDPA/Cu BS and DDPA/Cu AS was analyzed with a topomicroscope (Infinitefocus Alicona, Austria) composed of an optical microscope coupled to a camera. Unlike a confocal microscope, this microscope operated with a color contrast sensor. It generated topographic information combined with a color image from a stepped change in focus planes. Thereafter, the software reconstructed this information into an accurate set of data. It provided functionalities for dimensional measurements, characterization and surface analysis. Samples were placed on a motorized stage and illuminated by white light that could be modulated. Images were acquired continuously while the sample/objective distance was changed. With the lens selected, the image size was 143 $\mu\text{m} \times 109$ μm and the height resolution was 10 nm.

In addition to these measurements, the worn surfaces of the films were investigated with JSM-6400F scanning electron microscope.

3. Results and discussion

3.1. Characterization of Cu surface by XPS measurements and depth profile analyses

According to the widescan specific spectra of the chemical elements with all etching levels, (Fig. 1a–d) and the atomic percent profile (Fig. 1e), we can observe that:

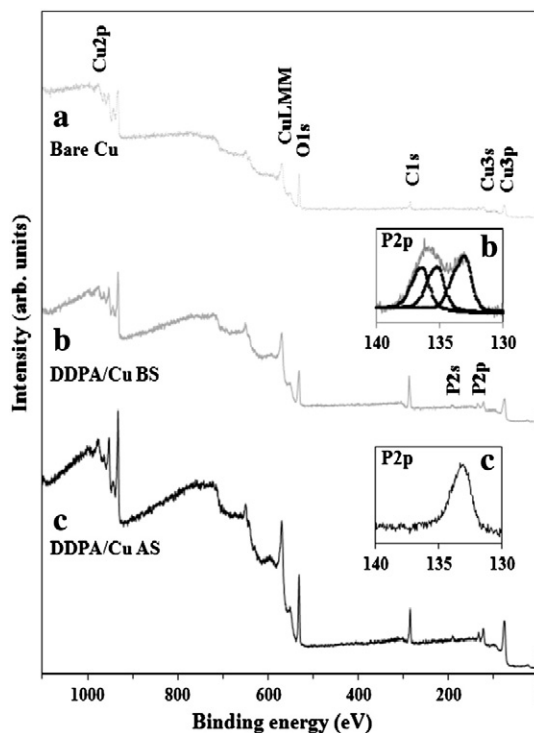


Fig. 2. Survey XPS spectra and enlarged region for P 2p peak for bare oxidized copper (a) and modified substrate with DDPA before (b) and after (b) sonication in absolute ethanol for 5 min.

- C 1s peak (Fig. 1a) appears at 285.5 eV, with 50% at the first level, increases from 50 to 60% at the second and the third level and then decreases fewer than 20% at the last level (Fig. 1e). It seems to show that there is a high thickness of atmospheric contamination at the surface of the sample. The deconvolution of this peak includes 2 contributions. The main one at 285.06 eV for C–H bindings and a smaller one at 1.89 eV higher than binding energy due to the C–O signal.
- O 1s peak (Fig. 1b) at 532 eV decreases slowly from 30% less than 0% from the first level to the last one (Fig. 1e). Oxygen peak shows two contributions, it seems to indicate that it is involved in C–O and Cu–O or Cu–(OH) bonds. On the second level of the oxygen analyzed, C–O contribution decreases and it disappears on the third level. It only stays on level 3 and level 4, the oxygen contribution corresponds to the CuO or Cu_2O bond. This contribution of oxygen was correlated to the evolution of the peak of auger Cu 2M2 at 565 eV (Fig. 1d).
- Cu 2p peaks (Fig. 1c) at 936 eV (Cu 2p_{3/2}) and 955.5 eV (Cu 2p_{1/2}), increase from 4% to more than 70% during etching (Fig. 1e).

Fig. 1c shows the first Cu 2p level with an evident binding to oxygen, as Cu 2p_{3/2} and Cu 2p_{1/2} doublet signal corresponds to Cu–O in CuO, Cu_2O or $\text{Cu}(\text{OH})_2$ compound [26]. After 400 s of etching, the metallic form of Cu appears [27]. The signal shows only two main bands

Table 1

The corresponding binding energy values for peak components of P 2p observed on modified substrate with DDPA before (DDPA/Cu BS) and after (DDPA/Cu AS) sonication in absolute ethanol for 5 min.

Peak components	Binding energy (eV)	
	DDPA/Cu AS	DDPA/Cu BS
P2p _{3/2}	132.9	133.0
P2p _{3/2}	–	135.1
P2p _{1/2}	133.9	133.9
P2p _{1/2}	–	136.1

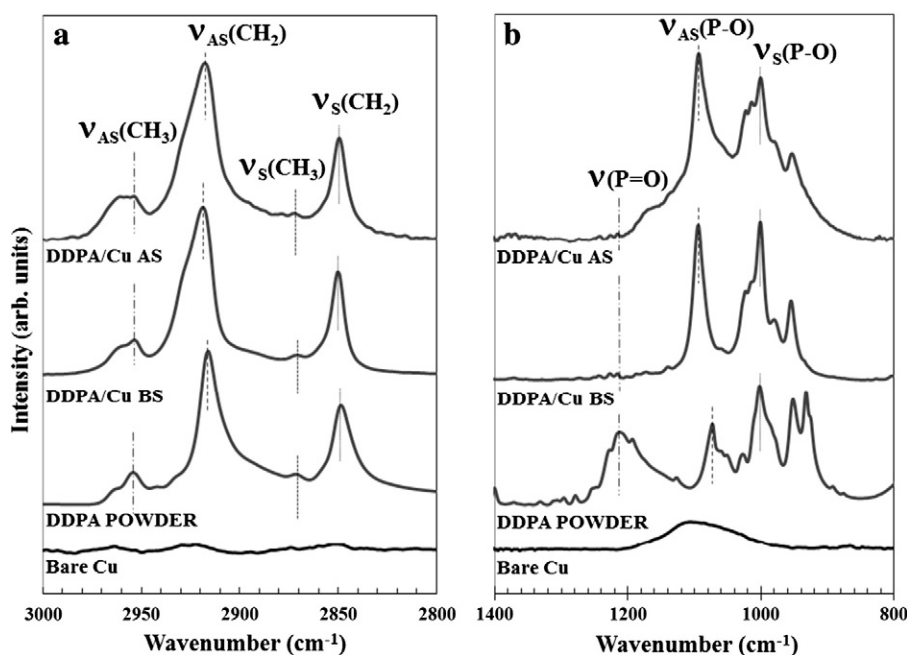


Fig. 3. PM-IRRAS spectrum of oxidized copper (Bare Cu), copper modified with DDPA before (DDPA/Cu BS) and after (DDPA/Cu AS) sonication and ATR-FTIR spectrum of DDPA powder (reference). The spectrum is presented in the high (A) and low (B) frequency regions.

at 933.5 eV and 953 eV, without any oxide contribution. From the second level to the last one, Cu 2p signal keeps the same.

Fig. 1d shows LM2 Auger peaks at 570 eV. The evolution of the Auger peak during the different levels of etching seems to indicate a decrease from 571.5 eV to 568 eV for the peak position and at the same time, the peak intensity increases from level 4 to the last one. The peak at 571.5 eV disappears progressively from level 1 to 4, and lets place to a high very thin peak at 568 eV. It is unexpected to notice that this transformation comes from level 4 to 5 and on the same sample, the oxidized states of Cu 2p were changing from level 1 to 2. It is probably due to three different states of oxidized copper, CuO, Cu₂O and Cu(OH)₂ at the surface of the substrate. This contribution of oxygen was correlated with the evolution of the peak of O 1 s oxygen at 532 eV, on Fig. 1b.

These analyses didn't show the presence of Phosphore element.

3.2. Characterization of SAM

Fig. 2 compares widescan XPS spectra of oxidized copper with the ones obtained from DDPA modified surface before and after sonication.

This step modifies significantly the surface composition. P 2p peaks, recorded before and after sonication (Fig. 2b and c, respectively) were quite different. When sonication was performed after modification, the phosphorus peak perfectly showed both states P 2p_{3/2} and P 2p_{1/2} (Table 1) corresponding to metallic junctions with the surface (binding energy of 133.9 and 132.9 eV, respectively) [3]. When no sonication was carried out after modification, two additional peaks appeared at 135.1 and 136.1 eV, respectively, corresponding to phosphorus weakly adsorbed on the substrate (Table 1). Therefore, ultrasonic cleaning is proved to remove physisorbed species, without any modification on chemisorbed ones.

Fig. 3 shows PM-IRRAS spectra of oxidized copper, copper modified with DDPA before and after sonication and DDPA powder as reference. Four bands were observed in the 2800–3000 cm⁻¹ region (Fig. 3A). When sonication was used, asymmetric CH₃ and CH₂ vibrations (ν_{AS}CH₃ and ν_{AS}CH₂) were located at 2955 cm⁻¹ and 2916 cm⁻¹ respectively, whereas symmetric CH₃ and CH₂ vibrations (ν_SCH₃ and ν_SCH₂) were found at 2871 and 2849 cm⁻¹, respectively (Table 2). These values were in accordance with good monolayer organization [4,5] and proved proper organization of DDPA SAMs grafted on copper

Table 2

Frequencies of the asym/sym functional groups vibrations of DDPA.

Wavenumber (cm ⁻¹)							
	ν _{AS} (CH ₃)	ν _{AS} (CH ₂)	ν _S (CH ₃)	ν _S (CH ₂)	ν(P=O)	ν _{AS} (P-O)	ν _S (P=O)
DDPA/Cu AS	2955	2916	2870	2848	–	1092	999
DDPA/Cu BS	2952	2918	2868	2849	–	1093	1000
DDPA powder	2951	2916	2869	2847	1206	1072	1001

Table 3

Contact angle and surface energy for different substrates.

Substrate type	Contact angle (°)				Surface energy (mJ·m ⁻²)		
	Water	Hexadecane	Methylene iodide	Bromonaphtalene	γ ^d	γ ^h	Total
Bare Cu	99 ± 5	5 ± 2	45 ± 5	39 ± 5	38.0	0.1	38.1
DDPA/Cu BS	129 ± 9	5 ± 2	79 ± 4	55 ± 2	20.7	1.2	21.9
DDPA/Cu AS	118 ± 1	5 ± 2	55 ± 9	60 ± 1	28.5	0.5	29.0

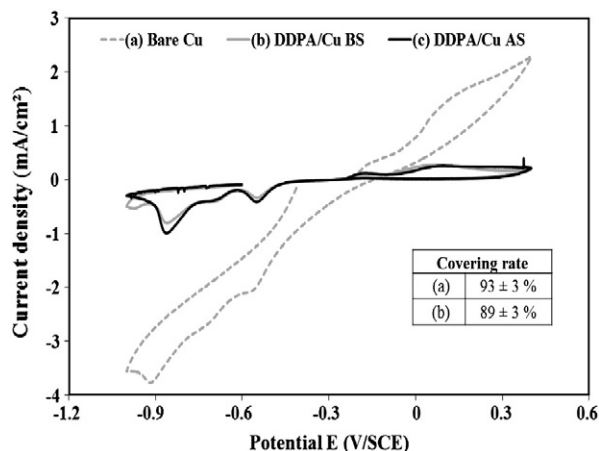


Fig. 4. Cyclic voltammograms of bare Cu electrode (curve a) and Cu modified electrode with DDPA before (curve b) and after (curve c) sonication in 0.1 M NaOH at room temperature and scan rate: 20 mV s^{-1} from -1 V/SCE to $+0.4 \text{ V/SCE}$. The values of recovery rate are also presented on the top right lower for a comparison.

in these conditions. Without sonication, the observed IR bands remained in accordance with good monolayer organization. Fig. 3B represented the region between 800 and 1400 cm^{-1} . The substrate oxidation was confirmed by a band in the $1200\text{--}1000 \text{ cm}^{-1}$ region correlated to the Cu-OH group, in addition to O-H band attributable to adsorbed water. The disappearance of bands attributed to $\nu\text{P=O}$ (1206 cm^{-1}) and $\nu\text{P-OH}$ (1072 cm^{-1}) [4], correlated to the appearance of a band at 1093 cm^{-1} corresponding to the P-O vibrations, proved the grafting mode of the molecule: the binding mode between phosphonic acid groups and oxidized copper substrate was probably tridentate [4].

Considering the macroscopic aspect, the effect of surface modification was quantified by measuring surface energies (Table 3). Compared to pretreated copper reference, the surface energy of functionalized surface was divided by two (21.9 vs. 38.1 mJ.m^{-2}). If sonication was used after modification, the value of the surface energy was a little higher but still well below the reference (29.0 mJ.m^{-2}). This result was in accordance with previous studies [2,3].

The covering rate was measured from cyclic voltammograms (Fig. 4). Good surface covering was observed. Ultrasound cleaning decreased slightly covering values (average value of 89% vs. 93%). However, it

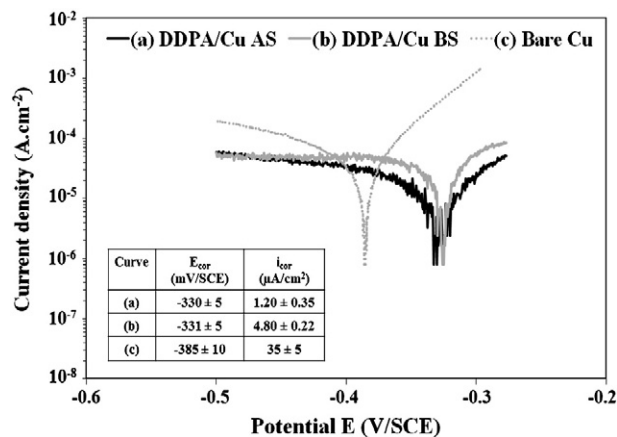


Fig. 6. Polarization curves for bare Cu substrate, Cu modified with DDPA before and after sonication (0.5 M aqueous NaCl, scan rate 5 mV s^{-1}). The values of corrosion potential and current rate are also presented on the table for comparison.

could be concluded that copper oxidation inhibition was high and similar in both cases (DDPA/Cu AS and DDPA/Cu BS).

Our results indicated that a well-organized and uniform phosphonic acid monolayer was clearly grafted onto pretreated copper surface. Fig. 5 shows the effect of ultra-sound cleaning on surface structure: it removes physically adsorbed species, consisting of small, uniformly distributed clusters of a few μm^2 , spaced from a few tens of μm as seen on SEM and optical microscope images. No such clusters appeared on the surface when sonication was used.

3.3. Anticorrosion properties of DDPA monolayers

Fig. 6 shows polarization curves and deduced values of corrosion current and potential. Very low values were observed for i_{cor} compared to reference surface (bare Cu). The corrosion current density i_{cor} decreased from $35 \mu\text{A/cm}^2$ for bare copper to $1.2 \mu\text{A/cm}^2$ when copper was modified with DDPA after sonication. Corrosion potential E_{cor} increased from -385 mV for bare copper to -330 mV for DDPA films. Both monolayers acted as corrosion inhibitors, as they greatly reduced copper corrosion rate and increased corrosion potential. Here again,

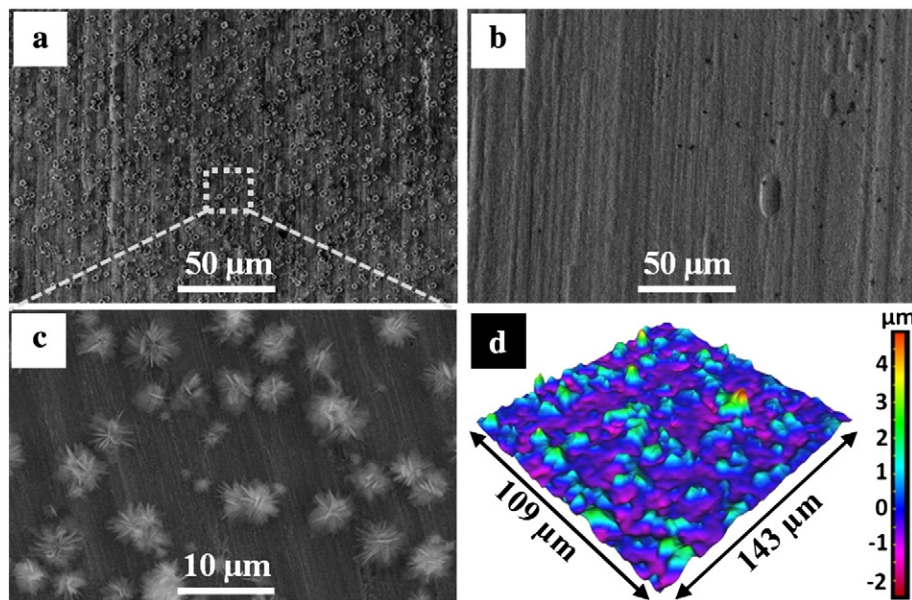


Fig. 5. SEM micrographs of DDPA/Cu surfaces before (a and c) and after (b) sonication and topographic optical microscope image of the DDPA/Cu BS (d).

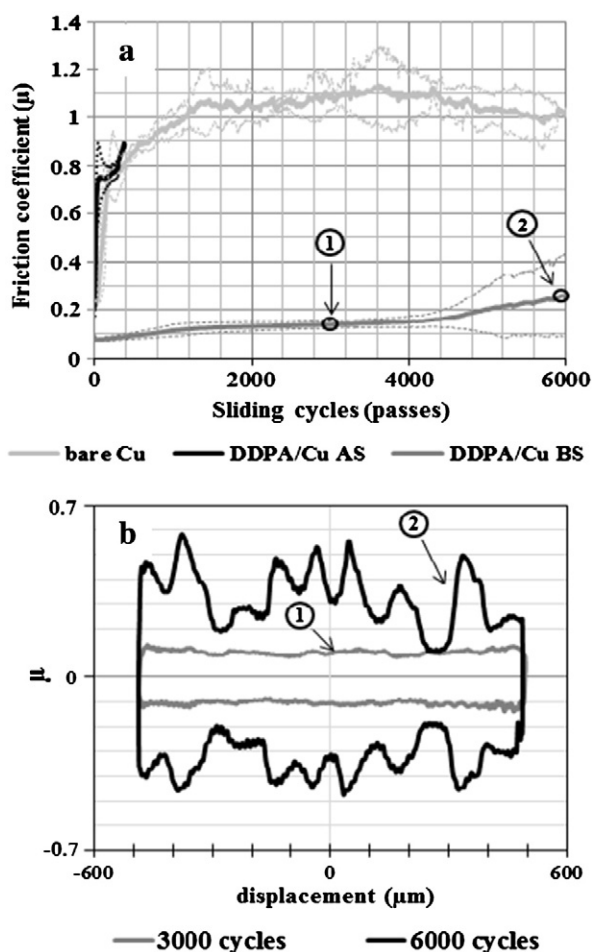


Fig. 7. Evolution of the mean friction coefficient, μ , ($\pm 500 \mu\text{m}$, 1 mm/s and 0.2 N) versus number of cycles (A). Dotted curves show standard deviation from few test results. The local evolution of the instantaneous friction coefficient for 3000 and 6000 specific cycle respectively of DDPA/Cu BS versus the position on the friction track (B). Each instantaneous friction coefficient curve is divided into two parts (positive and negative) because of the linear mode (two-way extraction).

DDPA molecular films were less efficient before than after sonication in terms of corrosion protection. This result supports the idea that a well-controlled interface and a well-organized organic monolayer are both needed for blocking efficiently the surface and obtaining a stable organic film. This result is identical to that demonstrated in former studies [14,15].

3.4. Tribological properties of monolayers

Fig. 7A presents the evolution of mean friction coefficient, μ , vs. sliding cycles, for bare Cu and Cu modified with DDPA before and after sonication.

Poor friction behavior was obtained in the case of bare Cu. It was also the case for tests performed with functionalized ultrasonic cleaned surface (DDPA/Cu AS). The mean friction coefficient started at 0.2 and reaches 0.8 after only 10 to 30 cycles. This indicates that metal adhesive junctions were quickly established, leading to seizure. In contrast, thin film of DDPA on copper substrate before sonication led to very low and stable value of friction coefficient ($\mu = 0.12$) and greatly increased the number of cycles before seizure (about 4000 cycles). This result is in accordance with previous study [28].

These results underline the negative effect of sonication treatment on the friction characteristics of films. As observed in Fig. 5, aggregates of a few μm^3 remain physisorbed on the surface before sonication treatment. Note that they are equally arranged on the surface with a density reaching approximately 25,000 aggregates per mm^2 . Obviously, these aggregates have a good influence on the tribological behavior, avoiding direct contacts and consequently local seizures.

While Fig. 7A shows the mean friction coefficient evolution along each whole cycle, the local evolution of the instantaneous friction coefficient μ vs. the position on the friction track could be observed on Fig. 7B. Indeed, the instantaneous friction coefficient surface of DDPA/Cu BS remained very low and constant up to 3000 sliding cycles. However, the repeated passage of the slider on the same track led to SAM removal on some surface spots. After 6000 cycles, some parts of the track led to $\mu > 0.5$, while others remained at a very low level of 0.1–0.2. So, the mean friction coefficient increased gradually, integrating part of increasing local SAM on the friction track. These micro-seizure spots led to widespread seizure after nearly 10000 cycles.

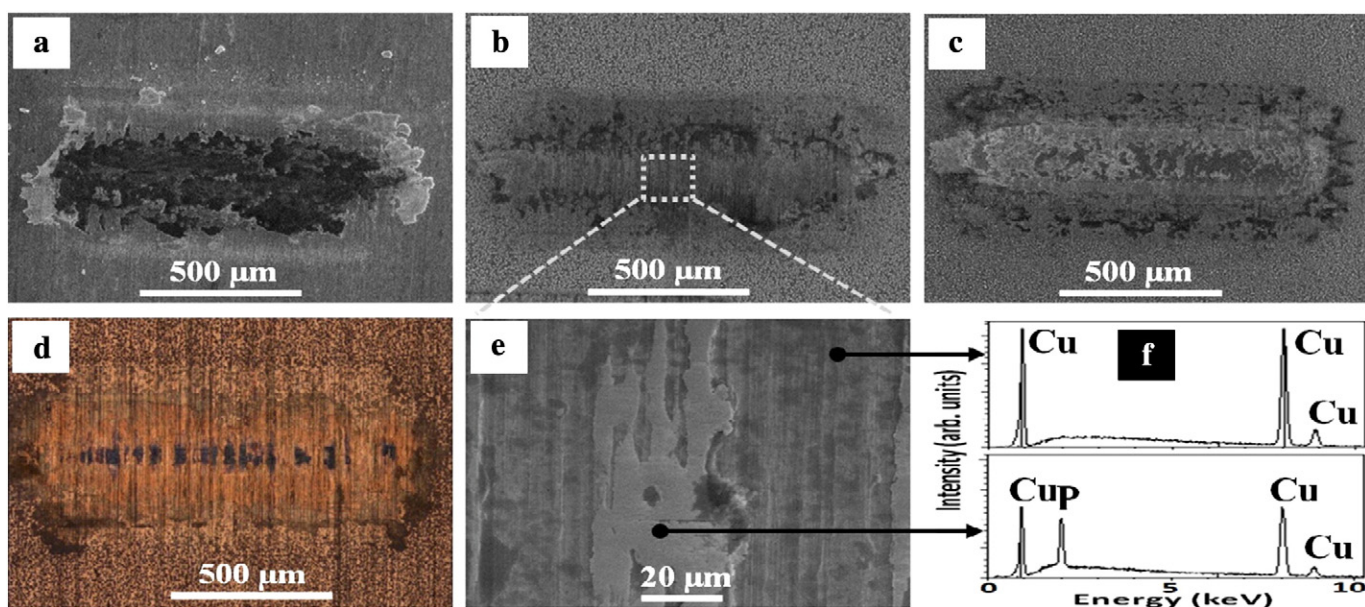


Fig. 8. (a) SEM micrographs of worn surfaces of bare copper sheet; and DDPA/Cu film before sonication (b and c) sliding against Si_3N_4 ceramic ball at 0.2 N and 1 mm/s for 3000 and 6000 cycles respectively. (d) Optical microscope image of worn surfaces of DDPA/Cu film before sonication sliding at 3000 cycles. (e) and (f) SEM micrograph and EDX analysis, respectively, from friction track of DDPA/Cu film before sonication at 3000 cycles.

These results were confirmed in Fig. 8, showing SEM micrographs of friction tracks and EDX analysis. Tracks appeared on bare copper after 6000 cycles (Fig. 8a) and on DDPA/Cu BS at 3000 and 6000 sliding cycles respectively (Fig. 8b and c). Surface became very rough and was characterized by severe adhesion wear, with some large wear particles appearing on the edges of the track. However, even after 6000 cycles performed (Fig. 8c), while no sonication was used after surface functionalization, the track included micro-seizure spots only on the bottom of the friction surface, where contact pressure was the largest. Moreover, EDX analyses (Fig. 8f) showed that there was phosphorus in some parts of the track, indicating that the monolayer was not completely removed.

These results underlined the dependence between the lubricating effect of DDPA monolayer and the presence of physisorbed molecule blocks not removed by sonication.

4. Conclusion

In this study, grafting quality (composition, structure and organization) of molecular films of n-dodecylphosphonic acid (DDPA) deposited on copper oxide was investigated. Corrosion resistance and tribological performance in terms of stability, friction decrease and anti-wear life were reported. Sonication of functionalized surface affects the grafting structure as evidenced.

The DDPA thin film was characterized using different techniques showing a well-organized grafting with good anti-corrosion properties.

XPS showed significant effects of ultrasonic cleaning on modified surface, i.e. removing of physisorbed species. SEM and topographic optical microscope images confirmed the presence of these small physisorbed molecule DDPA aggregates before sonication.

Results concerning the evolution of friction coefficient, SEM micrographs and EDX analysis of friction tracks proved the importance of physisorbed species on tribological behavior. Concerning DDPA/Cu BS surface, very high stability, low friction coefficient values (about 0.1) and a drastic increase of anti-wear life (100 times higher) were observed, compared to DDPA/Cu AS and unmodified Cu.

These promising results should focus further studies on modifying copper oxide surface by DDPA in metal forming processes. This work was partly supported by the french RENATECH network and its FEMTO-ST technological facility.

References

- [1] J.G. Van Alsten, *Langmuir* 15 (1999) 7605–7614.
- [2] E. Hoque, J.A. DeRose, G. Kulik, P. Hoffmann, H.J. Mathieu, B. Bhushan, *J. Phys. Chem.* 110 (2006) 10855–10861.
- [3] E. Hoque, J.A. DeRose, B. Bhushan, K.W. Hipps, *Ultramicroscopy* 109 (2009) 1015–1022.
- [4] G. Fonder, I. Minet, C. Volcke, S. Devillers, J. Delhalle, Z. Mekhalif, *Appl. Surf. Sci.* 257 (2011) 6300–6307.
- [5] M. Maxisch, C. Ebbert, B. Torun, N. Fink, T. de los Arcos, J. Lackmann, H.J. Maier, G. Grundmeier, *Appl. Surf. Sci.* 257 (2011) 2011–2018.
- [6] R. Bhure, T.M. Abdel-Fattah, C. Bonner, F. Hall, A. Mahapatro, *Appl. Surf. Sci.* 257 (2011) 5605–5612.
- [7] J. Wang, S. Yang, M. Chen, Q. Xue, *Surf. Coat. Technol.* 176 (2004) 229–235.
- [8] R. Hofer, M. Textor, N.D. Spencer, *Langmuir* 17 (2001) 4014–4020.
- [9] Y.T. Tao, *J. Am. Chem. Soc.* 115 (1993) 4350–4358.
- [10] R.R. Sahoo, S.K. Biswas, *J. Colloid Interface Sci.* 333 (2009) 707–718.
- [11] W.R. Thompson, J.E. Pemberton, *Langmuir* 11 (1995) 1720–1725.
- [12] Z. Mekhalif, F. Laffineur, N. Couturier, J. Delhalle, *Langmuir* 19 (2003) 637–645.
- [13] Z. Mekhalif, J. Delhalle, J.-J. Pireaux, S. Noël, F. Houzé, L. Boyer, *Surf. Coat. Technol.* 100–101 (1998) 463–468.
- [14] G. Fonder, F. Laffineur, J. Delhalle, Z. Mekhalif, *J. Colloid Interface Sci.* 326 (2008) 333–338.
- [15] T. Patois, A. Et Taouil, F. Lallemand, L. Carpentier, X. Roizard, J.-Y. Hihn, V. Bondeau-Patissier, Z. Mekhalif, *Surf. Coat. Technol.* 205 (2010) 2511–2517.
- [16] L.-K. Chau, M.D. Porter, *Chem. Phys. Lett.* 167 (1990) 198–204.
- [17] J.P. Folkers, C.B. Gorman, P.E. Laibinis, S. Buchholz, G.M. Whitesides, R.G. Nuzzo, *Langmuir* 11 (1995) 813–824.
- [18] D.L. Allara, R.G. Nuzzo, *Langmuir* 1 (1985) 45–52.
- [19] A. Ulman, *Chem. Rev.* 96 (1996) 1533–1554.
- [20] F. Schreiber, *Prog. Surf. Sci.* 65 (2000) 151–257.
- [21] F. Sun, D.G. Castner, D.W. Grainger, *Langmuir* 9 (1993) 3200–3207.
- [22] D.J. Dunaway, R.L. McCarley, *Langmuir* 10 (1994) 3598–3606.
- [23] N.E. Schlotter, M.D. Porter, T.B. Bright, D.L. Allara, *Chem. Phys. Lett.* 132 (1986) 93–98.
- [24] P.H. Mutin, G. Guerrero, A. Vioux, *Comptes Rendus Chimie* 6 (2003) 1153–1164.
- [25] D.K. Owens, R.C. Wendt, *J. Appl. Polym. Sci.* 13 (1969) 1741–1747.
- [26] In: D. Briggs, M.P. Seah (Eds.), *Auger and X-ray Photoelectron Spectroscopy*, Volume 1, John Wiley & Sons, 1996.
- [27] T. Ghodselahe, M.A. Vesaghi, A. Shafiekhani, A. Baghizadeh, M. Lameii, *Appl. Surf. Sci.* 255 (2008) 2730–2734.
- [28] Y. Wana, Y. Wanga, Q. Zhanga, Z. Wanga, Z. Xua, C. Liua, J. Zhang, *Surf. Coat. Technol.* 259 (2012) 147–152.